Permeation and Interaction of Divalent Cations in Calcium Channels of Snail Neurons

LOU BYERLY, P. BRYANT CHASE, and JOSEPH R. STIMERS

From the Department of Biological Sciences, University of Southern California, Los Angeles, California 90089

ABSTRACT We have studied the current-carrying ability and blocking action of various divalent cations in the Ca channel of *Lymnaea stagnalis* neurons. Changing the concentration or species of the permeant divalent cation shifts the voltage dependence of activation of the Ca channel current in a manner that is consistent with the action of the divalent cation on an external surface potential. Increasing the concentration of the permeant cation from 1 to 30 mM produces a twofold increase in the maximum Ca current and a fourfold increase in the maximum Ba current; the maximum Ba current is twice the size of the maximum Ca current for 10 mM bulk concentration. Correcting for the changing surface potential seen by the gating mechanism, the current-concentration relation is almost linear for Ba^{2+}, and shows only moderate saturation for Ca^{2+}; also, Ca^{2+}, Ba^{2+}, and Sr^{2+} are found to pass through the channel almost equally well. These conclusions are obtained for either of two assumptions: that the mouth of the channel sees (*a*) all or (*b*) none of the surface potential seen by the gating mechanism. Cd^{2+} blocks *Lymnaea* and *Helix* Ca channels at concentrations 200 times smaller than those required for Co^{2+} or Ni^{2+}. Ca^{2+} competes with Cd^{2+} for the blocking site; Ba^{2+} binds less strongly than Ca^{2+} to this site. Mixtures of Ca^{2+} and Ba^{2+} produce an anomalous mole fraction effect on the Ca channel current. After correction for the changing surface potential (using either assumption), the anomalous mole fraction effect is even more prominent, which suggests that Ba^{2+} blocks Ca current more than Ca^{2+} blocks Ba current.

INTRODUCTION

This paper characterizes the permeation mechanism of the Ca conductance in *Lymnaea* neurons. We were initially prevented from doing these experiments with the internal perfusion technique because the Ca current rapidly washed out of well-perfused neurons (Byerly and Hagiwara, 1982). We have found that the Ca current is much more stable if the perfusion is limited by using suction

Address reprint requests to Dr. Lou Byerly, Dept. of Biological Sciences, University of Southern California, Los Angeles, CA 90089. Dr. Stimers' present address is Dept. of Physiology, UCLA Medical School, Los Angeles, CA 90024.

J. GEN. PHYSIOL. © The Rockefeller University Press · 0022-1295/85/04/0491/28 $1.00

Volume 85 April 1985 491–518

electrodes with a small tip diameter (~1/10 the diameter of the cell). With such poorly perfused cells, it is possible to examine the concentration dependence, selectivity for permeant ions, and blocker sensitivity of the Ca channel, while permitting the replacement of internal K^+ with Cs^+ in ~15 min.

The development of a model for the Ca channel permeation mechanism has been complicated considerably by the strong interactions of divalent cations with the membrane surface charge. Hagiwara and Takahashi (1967) conducted the first thorough study of Ca channel permeation using barnacle giant muscle fibers. They introduced a one-site model that successfully accounted for both permeation and blocking by various divalent cations. Surface potential variation was apparently avoided in this study by the presence of high concentrations of Mg^{2+}. In subsequent studies of Ca currents in other tissues, increases in the Ca^{2+} concentration shifted the activation of the Ca current to more positive potential, as would be expected if a substantial negative surface charge was present. In many of these studies, the possible presence of a changing surface potential was ignored and the observed saturation of the Ca current with increasing Ca^{2+} concentration was attributed entirely to binding of Ca^{2+} to a site on the channel. Ohmori and Yoshii (1977) studied the Ca current of tunicate eggs and interpreted the shifts in activation as changes in the surface potential. Assuming that the channel opening saw the same surface potential changes, they concluded that the Ca channel current was proportional to the permeant ion concentration and showed no indication of binding to a channel site. Using similar assumptions, Wilson et al. (1983) reached the same conclusion for the Ca channel of the snail *Helix*, and Cota and Stefani (1984) found that some (but not all) of the saturation observed in the Ca current of frog skeletal muscle could be explained by the effect of surface potential on the concentration of Ca^{2+} at the channel opening.

Hess et al. (1983) reported an anomalous mole fraction effect for the Ca channel current of heart muscle, which was accounted for by a two-site model (Hess and Tsien, 1984). Almers and McCleskey (1984) found a similar effect for the Ca current of frog skeletal muscle and described it by a similar model. These studies did not consider the possible presence of surface potential changes. One of the purposes of the studies described here was to determine if surface potential corrections might be able to account for the anomalous mole fraction effect.

In our studies on *Lymnaea*, we found that corrections for surface potential produce results very similar to those of Ohmori and Yoshii (1977) and Wilson (1983), except for some indication of binding to a channel site in the current-concentration relationships (as in Cota and Stefani, 1984). We found that *Lymnaea* and *Helix* Ca channels have the same sensitivity to blockers and that there is competition between blocking and permeant ions, even after surface potential corrections. We also found an anomalous mole fraction effect, which becomes even more prominent after surface potential corrections.

METHODS

All experiments were done with the internal perfusion voltage-clamp technique on isolated nerve cell bodies, following the methods of Byerly and Hagiwara (1982). Most of the nerve cells studied were from the snail *Lymnaea stagnalis*, but a few cells from the snail *Helix aspersa* were used in the blocker studies. Our technique had a much lower success

rate for providing healthy isolated cells from *Helix* than from *Lymnaea*. We studied unidentified cells of 80–140 μm diam from the subesophageal ganglia in both species.

Types of Experiments

The experimental procedures used fall into four types, determined by the extent of internal perfusion, the method for recording transmembrane potential, and the temperature. Since most of these studies required relatively stable Ca channel currents, three of the types of experiments were designed to slow down Ca current washout, either by a greatly limited rate of internal perfusion or by low temperature. In all experimental types, the bath was held at virtual ground by the current-to-voltage converter used to record membrane current. This also served as the reference for recording transmembrane potential. The four types of experiments are as follows.

PERMEATION EXPERIMENTS This type of experiment was used for studies of the dependence of the magnitude of the Ca channel current on the composition of the external solution, except for some of the blocker studies (see below). The opening of the suction electrode that seals to the cell (and carries the internal solution) was only 10–15 μm in diameter. With these small-opening suction electrodes, intracellular K^+ is replaced by Cs^+ in ~15 min and the Ca current is typically reduced by <20% after 1 h of perfusion (Byerly and Hagiwara, 1982). The high series resistance of these small suction electrodes (0.5–1.5 MΩ) makes the potential recorded inside the suction electrode significantly different from the intracellular potential when large currents pass through the suction electrode; therefore, the intracellular potential was directly measured by a 3 M KCl microelectrode inserted into the cell. The potential recorded by this microelectrode was the feedback signal for the voltage-clamp amplifier. These experiments were done at room temperature to give large Ca channel currents (Byerly et al., 1984*a*).

BLOCKER EXPERIMENTS These experiments were the same as the permeation experiments except that a separate microelectrode was not used. The potential recorded inside the suction electrode was clamped, with the use of electronic compensation for series resistance errors. Because of its technical simplicity, this type of experiment was used for some blocker studies in which the peak magnitude, but not the voltage dependence, of the current was of interest. Control experiments demonstrated that permeation and blocker measurements done on the same cell gave identical values for the peak magnitude of the current.

TAIL CURRENT EXPERIMENTS This type of experiment is the same as that recently described by Byerly et al. (1984*a*). The Ca tail current is resolved by speeding up the clamp (large-opening suction electrode and low-resistance recording microelectrode in the cell) and by slowing down the Ca channel kinetics by working at low temperatures (7–10°C). In spite of the large suction electrode opening (diameter equal to one-third the cell diameter), the Ca current washout is slow at low temperatures (Byerly et al., 1984*a*).

REVERSAL EXPERIMENTS This type of experiment was used to look for a reversal of the Ca channel current. Since these experiments do not require long-term stability of the Ca current, the experiments could be done at room temperature with large-opening suction electrodes. Suction electrodes with large openings were necessary in these experiments to raise the intracellular pH (Byerly and Moody, 1982); at pH 8.2, the H^+ current (Byerly et al., 1984*b*), which overlaps the Ca current, is greatly reduced. The suction electrode potential was clamped (with series resistance compensation) in these experiments; this provided good control of the intracellular potential since the resistance of the suction electrode was small (200–400 kΩ) and the currents were small at the potentials of interest.

In the permeation and tail current experiments, the current and voltage records were digitized with 12-bit resolution at intervals of 50 (permeation) or 20 μs (tail current). The current was filtered by a 10- (tail current) or 3-kHz (other types) low-pass circuit. The

pulse duration was 30 ms in permeation experiments and 10 ms in tail current experiments. Immediately after the positive pulse, a pulse of equal amplitude and opposite polarity was applied to the voltage command. The currents recorded from the positive and negative pulses were summed to eliminate linear leakage and capacitive currents. These summed currents were stored on a floppy disk for later analysis.

In the blocker and reversal experiments, the current records were photographed from the screen of a storage oscilloscope and measurements were taken from the film. The pulse duration was 60 ms in these experiments. Currents from negative pulses were recorded for blocker experiments to allow manual subtraction of linear leakage currents. No such correction was made in reversal experiments, because nonlinear background currents were much larger than the linear leakage at the potentials of interest.

Solutions

Table I gives the compositions of the external and internal solutions. Neither external nor internal solutions contained ions that are appreciably permeant through K or Na channels, and 10 mM 4-aminopyridine (4-AP) was added to all external solutions to

TABLE I

Compositions of Solutions

External solutions	Ca^{2+}	Mg^{2+}	HEPES	Tris	4-AP
	mM	*mM*	*mM*	*mM*	*mM*
1 mM Ca saline	1	0	10	76	10
3 mM Ca saline	3	0	10	72	10
10 mM Ca saline	10	0	10	62	10
30 mM Ca saline	30	0	10	27	10
Tris saline	4	4	0	65	10
Helix Tris saline	10	4	0	128	10

Internal solutions	Cs^{+}	Aspartate	HEPES	TAPS	EGTA
	mM	*mM*	*mM*	*mM*	*mM*
Cs-aspartate	74	62	5	0	5
pH 8.2 Cs-aspartate	74	28	0	100	5
Helix Cs-aspartate	148	117	10	0	10

suppress H^{+} currents (Byerly et al., 1984*b*). Therefore, the currents recorded during perfusion with these solutions should primarily pass through the Ca channel, especially at potentials of <20 mV. All external solutions were made from chloride salts and adjusted to pH 7.4 with HCl. The pH of the normal internal solution, Cs-aspartate, was 7.3, but pH 8.2 Cs-aspartate solution was used in the study of reversal potentials to further reduce H^{+} currents. The pH of the *Helix* Cs-aspartate solution was 7.4.

When Ba^{2+} or Sr^{2+} was used as the permeant ion, it replaced Ca^{2+} in the solutions given in Table I. The mixtures of Ba^{2+} and Ca^{2+} used in demonstrating the anomalous mole fraction effect were obtained by mixing appropriate ratios of the 10 mM Ca saline and 10 mM Ba saline. In studies of the blocking actions of Cd^{2+}, Co^{2+}, and Ni^{2+}, the chloride salts were added directly to the external solutions given in Table I, without adjusting the concentrations of other ions. A 10-mM solution of nifedipine (Sigma Chemical Co., St. Louis, MO) in ethanol was diluted by a factor of 100 in 3 mM Ca saline, giving 10^{-4} M nifedipine and 1% ethanol. Lower concentrations of nifedipine were obtained by diluting this 10^{-4} M solution in 3 mM Ca saline containing 1% ethanol. Nifedipine-containing

solutions were stored in the dark, and experiments with these solutions were done under dim light. External solutions used with the pH 8.2 Cs-aspartate internal solution were made hyperosmotic by adding 60 mM glucose to compensate for the high osmolarity produced by 100 mM tris(hydroxymethyl)methylaminopropane sulfonic acid (TAPS).

Procedures

For an examination of the dependence of the magnitude of the Ca channel current on the concentration or species of the permeant ion, *I-V* relations were determined for the control solution before and after the measurements in each of the other solutions tested. This allowed a correction for slow washout of the Ca channel current and rejection of data when an irreversible change occurred in membrane properties. The control solution for the studies of dependence on permeant ion concentration was the solution containing 3 mM of the permeant ion; the control solution for the studies of dependence on permeant ion species was the 10 mM Ca saline. If the magnitude of the control *I-V* relation dropped by ≥30% from its previous value, or if V_a, the potential of half-maximum current, changed by more than a few millivolts, the data were discarded. When the control *I-V* curves were in satisfactory agreement, the test solution values were compared with the mean for those of the two control *I-V* curves. In a typical experiment, *I-V* curves were measured for two or three test solutions along with three or four measurements of the *I-V* curve for the control solution. The *I-V* curve measured in the control solution tended to shift to more positive potentials as the experiment progressed. The last *I-V* curve measured was sometimes shifted by as much as 10 mV from the first *I-V* curve. The mean shift of V_a in 16 experiments was 4.0 ± 2.6 mV (± SD) in the positive direction.

During experiments in which the potential recorded by the intracellular microelectrode was clamped, the DC level of the command voltage was adjusted as necessary (at 1-min intervals) to keep the potential recorded inside the suction electrode constant at the holding potential. At the holding potential, the suction electrode potential and the intracellular potential should be essentially equal, since the holding current is small (typically <1 nA). The change in potential recorded by the microelectrode on impalement was equal to the measured suction electrode potential; the difference between these two values for 15 impalements was 0.0 ± 2.4 mV (mean ± SD). However, the microelectrode potential frequently drifted 10–15 mV negative relative to the suction electrode potential during the course of an experiment. Tests at the end of the experiment showed that the microelectrode had "clogged," while the potential of the suction electrode in the reference solution (without the cell) was unchanged from the beginning of the experiment. The greater stability of the suction electrode potential measurement is not surprising given the much lower resistance (<1 MΩ) of the 3 M KCl electrode in the suction electrode compared with the 4–10-MΩ resistance of the intracellular microelectrode. Consequently, the suction electrode potential was always accepted as the correct measurement of the holding potential, even though the intracellular microelectrode potential was superior for controlling the voltage steps because of the large reduction in series resistance.

In blocker experiments, the Ca channel current was measured first in the absence of blocker and then in the presence of increasing concentrations of the blocker. After the measurement in the highest concentration of blocker, the cell was washed for several minutes in blocker-free solution. Usually only about half of the Ca channel current returned. We assume that the partial reversal was due to the difficulty in completely removing the tightly binding blocker ions. Since measurements in six concentrations of blocker could be finished in <20 min, very little Ca current washout would be expected in these poorly perfused cells. For these reasons, we compared the currents measured in the presence of blocker with those measured before the blocker, rather than after. The

return of the Ca current after the blockers was much more complete for *Helix* cells than *Lymnaea* cells, perhaps because of the higher concentration of Ca^{2+} in the *Helix* saline.

RESULTS

Dependence of Current on External Concentration of Permeant Ion

EFFECTS OF DIVALENT IONS ON SURFACE POTENTIAL We assume that the the magnitude of the inward current passing through an open Ca channel depends on the concentration of the permeant ion M^{2+} at the external opening of the channel, $[M^{2+}]_C$, and the potential difference across the channel, V_C. We assume that the concentration of M^{2+} at the internal end of the channel is zero, since all experiments were done under conditions where the internal concentration of divalents was probably very low (Byerly and Moody, 1984). If the external surface of the channel has a surface charge density σ, there is a surface potential ϕ_O that will determine the relation between the variables relevant to the channel, $[M^{2+}]_C$ and V_C, and those that are measured, $[M^{2+}]_O$ and V_M. $[M^{2+}]_O$ is the concentration of M^{2+} in the bulk solution outside the cell and V_M is the measured membrane potential. $[M^{2+}]_C$ is calculated from the Boltzmann relation:

$$[M^{2+}]_C = [M^{2+}]_O \exp(-2F\phi_O/RT), \quad (1)$$

and V_C is given by

$$V_C = V_M - \phi_O + \phi_I, \quad (2)$$

where ϕ_I is the internal surface potential. Note that throughout this study we use concentrations where activities should be used (e.g., Eq. 1). The uncertainties in calculating single-ion activities for divalent cations have caused us to follow this practice, which was also followed in most previous studies of Ca channel permeation.

Since the surface potential ϕ_O is strongly dependent on $[M^{2+}]_O$, both the number of open channels and V_C usually change with $[M^{2+}]_O$, even when V_M is constant. Hagiwara and Takahashi (1967) tried to eliminate this complication by keeping 100 mM Mg^{2+} in all solutions and found that the threshold of the barnacle muscle action potential no longer varied with the concentration of the permeant ion. However, in other cells, including snail neurons, it is not possible to avoid changes of the surface potential by working with a high concentration of Mg^{2+} in the bathing solution (Ohmori and Yoshii, 1977; Wilson et al., 1983). Even with 33 mM Mg^{2+} in the external solutions, we found that changing from 10 mM Ca^{2+} to 10 mM Ba^{2+} caused the *I-V* curve measured for the *Lymnaea* divalent current to shift ~15 mV in the negative direction. Therefore, the dependence of I_M on $[M^{2+}]_C$ at constant V_C can only be determined in the presence of changing surface potential and corresponding corrections must be made.

The change of surface potential seen by the gating mechanism as $[Ca^{2+}]_O$ was changed to 1, 3, 10, and 30 mM was determined from the voltage dependence of activation of the Ca current, as determined from tail currents. The amplitude of the tail current measured at −50 mV was plotted against the potential of the pulse that activated the Ca channel (Fig. 1 *A*). The Ca current is seen to activate

at more positive potentials as $[Ca^{2+}]_o$ increases. The arrows in Fig. 1 *A* indicate the potentials at which half of the Ca channels are activated, V_{at}. Taking 3 mM Ca^{2+} as the reference, the change in V_{at} was determined for the other concentrations of Ca^{2+} (Fig. 1 *B*). Interpreting these ΔV_{at} values as reflecting changes in

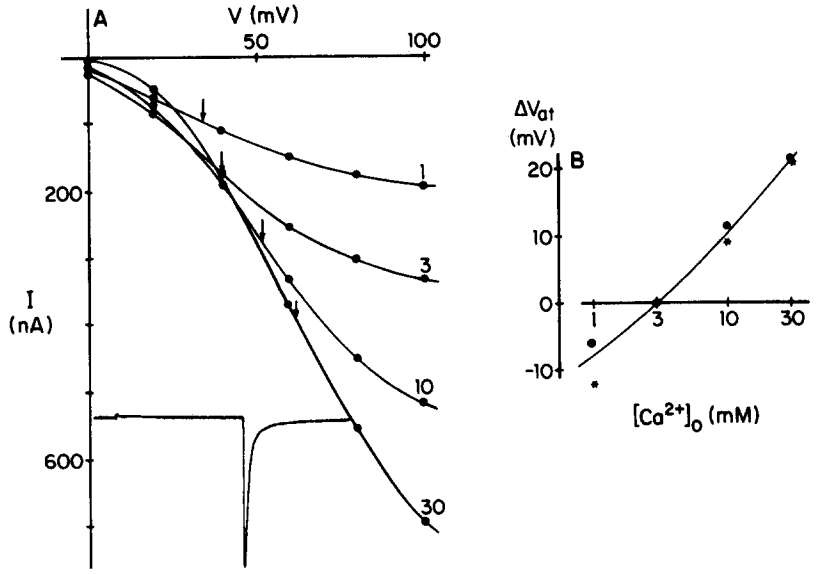

FIGURE 1. Dependence of Ca current activation on external Ca^{2+} concentration. Tail current experiment: large-opening suction electrode, intracellular microelectrode, 7–10°C. The activating prepulse was 10 ms in duration and tail currents were measured at the holding potential (−50 mV). The internal solution was Cs-aspartate; external solutions were 1, 3, 10, and 30 mM Ca salines. The inset in *A* shows the current record for the prepulse to 100 mV with 30 mM Ca saline; the peak tail current is −700 nA. (*A*) Tail current amplitude plotted against prepulse potential. The tail current amplitude is measured at its peak (~200 μs from beginning of the step down in potential; see inset). Numbers by curves indicate the Ca^{2+} concentration (millimolar). Since each of the four *I-V* curves was assumed to have the same sigmoidal shape, the maximum current at large positive potentials was calculated from the maximum slope for each curve and the ratio of maximum slope to current at 100 mV for the 1 mM Ca saline. The potential at which the tail current is one half of the maximum current, V_{at}, is indicated by an arrow for each curve. (*B*) Shift of V_{at} vs. Ca^{2+} concentration. Shifts of V_{at} are measured relative to V_{at} for 3 mM Ca saline. Data are from the cell of part *A* and another cell. The curve is the same as that drawn through the data of Fig. 2 *B*.

the surface potential, increasing $[Ca^{2+}]_o$ from 1 to 30 mM increases the surface potential by 30 mV.

The *I-V* relations measured for the peak Ca current during the voltage pulse show the same shifts in voltage dependence with changes in $[Ca^{2+}]_o$ that were determined from the tail current activation curves. Fig. 2 *A* shows the *I-V* curves

measured for the peak inward current in 1, 3, 10, and 30 mM Ca^{2+} solutions. The arrows indicate the potentials at which half of the maximum current is recorded, V_a, for each $[Ca^{2+}]_o$. The change in V_a produced by a change in $[Ca^{2+}]_o$ (Fig. 2*B*) is the same as that determined from the tail currents (Fig. 1*B*); the curve drawn through the data in Fig. 2*B* is reproduced in Fig. 1*B*, where it is in

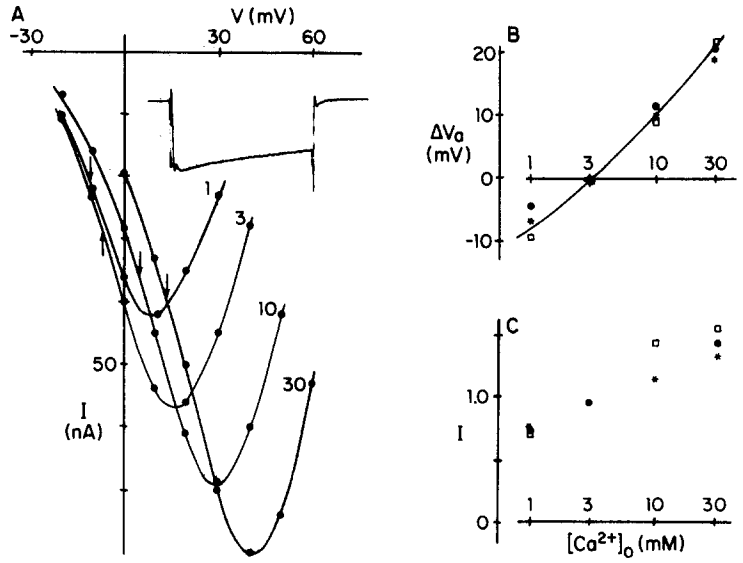

FIGURE 2. Dependence of the peak Ca current on external Ca^{2+} concentration. Permeation experiment: small-opening suction electrode, intracellular microelectrode, room temperature. The pulse duration was 30 ms and the holding potential was −50 mV. The internal solution was Cs-aspartate; external solutions were 1, 3, 10, and 30 mM Ca salines. The inset in *A* shows the current record for the pulse to +30 mV with 30 mM Ca saline; the peak Ca current is −70 nA. The underdamped quality of clamp was due to the high resistance of the small-opening suction electrode. (*A*) Peak Ca current plotted against the pulse potential. The largest inward current recorded during each pulse was measured. Numbers by the curves indicate the Ca^{2+} concentration (millimolar). The potential at which the peak current is one half of the maximum peak current, V_a, is indicated by an arrow for each curve. (*B*) Shift of V_a vs. Ca^{2+} concentration. Shifts of V_a are measured relative to the V_a for 3 mM Ca saline. Data from three cells are plotted with different symbols. Filled circles are used for data from part *A*. The curve is drawn by eye through the data and is reproduced in Fig. 1*B*. (*C*) Ca current at $V_a + K$ vs. Ca^{2+} concentration. K is a constant for any one cell and is ~20 mV; K is chosen such that $V_a + K$ is close to the potential at which the maximum current occurs for each concentration of Ca^{2+}. Currents are normalized to the current for the 3 mM Ca saline.

good agreement with the data. This agreement is remarkable considering that V_a is 45–50 mV more negative than V_{at} and corresponds to the opening of <5% of the Ca channels. The voltage dependence of the Ca current measured during the pulse is a product of two terms, a gating term that expresses the voltage dependence of activation of channels and a permeation term that expresses the

I-V relation for open Ca channels. If it is assumed that the permeation mechanism of the channel sees the same V_C as does the gating mechanism and that the concentration of permeant ions inside the cell is negligibly small, the Ca current *I-V* curve (Fig. 2) would be expected to shift by the same amount as the activation curve (Fig. 1) when the surface potential changes. Given the good agreement between Figs. 1*B* and 2*B*, we interpret the shifts measured in V_a determined from ordinary *I-V* curves as the changes in the surface potential seen by the Ca channel gating mechanism.

When the permeant ion is Ba^{2+} instead of Ca^{2+}, the value of V_a shifts 25 mV in the positive direction as the concentration of Ba^{2+} is increased from 1 to 30 mM (Fig. 3). However, the V_a values are 10–15 mV more negative for Ba current than for Ca current, which we interpret to mean that Ca^{2+} binds more readily to the negative surface charge than does Ba^{2+}. In the absence of evidence to the contrary and in accordance with the conclusions of others in studies on artificial phospholipid membranes (McLaughlin et al., 1971), tunicate egg cell membrane (Ohmori and Yoshii, 1977), and snail neuron membrane (Wilson et al., 1983), we assume that Ba^{2+} does not bind to the surface charge, but changes the surface potential ϕ_O only through a screening action. The Grahame equation relates ϕ_O to σ as follows:

$$(G\sigma)^2 = \sum_i C_i[\exp(-z_i F\phi_O/RT) - 1]. \quad (3)$$

The sum is taken over all species of ions present in the external solution; z_i and C_i are the valence and concentration of the ion of species i, and G is a constant equal to ~270 Å^2 (electronic charge)$^{-1}$ (mol/liter)$^{-1/2}$ at the temperature of our experiments. The solid smooth curve drawn in Fig. 3*B* shows the fit to the Ba data that we obtained with the Grahame equation. All species of external ions were included in these calculations, since $Tris^+$ exerts even more screening than does Ba^{2+} in the solutions of lower $[Ba^{2+}]$. This fit gives a σ of 1 electronic charge/206 Å^2 (14.3 Å between charges) and a ϕ_O of −69.5 mV in 3 mM Ba saline. This value for surface charge density is intermediate between two values recently calculated for *Helix* neurons—21 Å (Kostyuk et al., 1982) and 9 Å between charges (Wilson et al., 1983). Dashed curves show the relations that are obtained if ϕ_O for 3 mM Ba saline is increased or decreased by 10 mV; these relations are clearly inconsistent with the data. The estimated error in σ is ±5%.

As further evidence to support our interpretation of the shifts in the voltage dependence of activation reported above to indicate changes in surface potential, we point out the following previously published results concerning activation of divalent current in the cells. The currents recorded during activating voltage pulses (inset, Fig. 2*A*) show very little inactivation. The rate of activation is at least two orders of magnitude faster than that of inactivation (Byerly and Hagiwara, 1982); therefore, changes in the rate of inactivation that might be expected with changes in current magnitude or permeant ion species (Brehm and Eckert, 1978; Tillotson, 1979) would have very little effect on the peak currents measured. Also, it has been shown that the time courses of both activation and deactivation (tail currents) are the same for Ca currents as for Ba currents when the 10–15-mV shift in surface potential noted above is taken into

account (Byerly and Hagiwara, 1982; Byerly et al., 1984*a*). Thus, there is no evidence of divalent cations affecting the activation kinetics of these Ca channels directly, i.e., independently of surface potential changes.

DEPENDENCE OF CURRENT ON SURFACE CONCENTRATION OF PERMEANT ION We do not know how much of the surface potential is seen by the

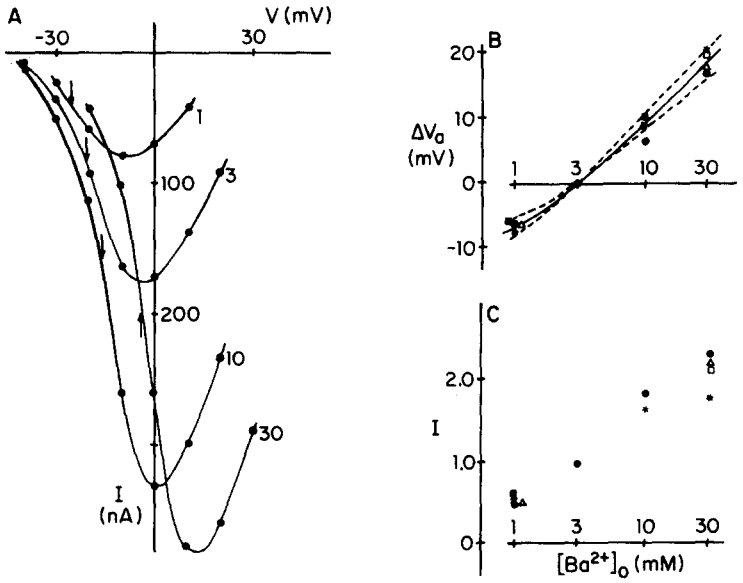

FIGURE 3. Dependence of the peak Ba current on external Ba^{2+} concentration. Permeation experiment: small-opening suction electrode, intracellular microelectrode, room temperature. The pulse duration was 30 ms and the holding potential was −50 mV for all solutions. The internal solution was Cs-aspartate; external solutions were 1, 3, 10, and 30 mM Ba salines. Later studies showed that the Ba current was slightly inactivated in 1 mM Ba saline with a holding potential of −50 mV. With a holding potential of −70 mV or a more negative value, the magnitude of the Ba current in 1 mM Ba saline was 10% greater than that recorded with a holding potential of −50 mV, but there was no shift in voltage dependence. No correction has been made for this inactivation, since the cell-to-cell scatter in the data is >10%. (*A*) Peak Ba current plotted against the pulse potential. The largest inward current recorded during each pulse was measured. Numbers by the curves indicate Ba^{2+} concentration (millimolar). The potential at which the peak current is one half of the maximum peak current, V_a, is indicated by an arrow for each curve. (*B*) Shift of V_a vs. Ba^{2+} concentration. Shifts of V_a are measured relative to the V_a for 3 mM Ba saline. Data from five cells are plotted with different symbols. The curves are drawn according to Grahame equation (Eq. 3). The solid curve corresponds to a surface potential of −69.5 mV for 3 mM Ba saline; the dashed curves correspond to surface potentials 10 mV larger or smaller. (*C*) Ba current at $V_a + K$ vs. Ba^{2+} concentration. K is a constant for any one cell and is ~20 mV; K is chosen such that $V_a + K$ is close to the potential at which the maximum current occurs for each concentration of Ba^{2+}. Currents are normalized to the current for 3 mM Ba saline.

permeation mechanism. Although the mouth of the channel may see the same surface potential changes that are seen by the gating mechanism, it is certainly possible that the changes seen by the mouth of the channel are smaller (or greater) than those felt by the gating mechanism (Begenisich, 1975). The Debye length for these solutions is 10–12 Å. We consider two assumptions in analyzing our data: (*a*) the mouth of the channel sees the same ϕ_O that was determined from the gating, so that Eq. 1 relates $[M^{2+}]_C$ and $[M^{2+}]_O$, and (*b*) the mouth of the channel sees none of the surface potential, i.e., $[M^{2+}]_C = [M^{2+}]_O$. We favor the first assumption somewhat, since it is consistent with the result demonstrated in Figs. 1 and 2 that the *I-V* curve for the peak Ca current during the pulse shows the same shifts in potential that the activation curve does (measured from tail currents). Ohmori and Yoshii (1977) have shown that assumption *a* allows a very satisfactory explanation of the effects of divalent cations on the magnitudes of currents through both Na and Ca channels in tunicate egg cell membrane. However, it will be shown that both assumptions give qualitatively similar results, so that we can reach certain conclusions without knowing which assumption is closer to the truth.

First we consider assumption *a*, that the permeation mechanism of the Ca channel sees the same transmembrane potential, V_C, that the gating mechanism does, so the concentration of the permeant ion at the mouth of the channel, $[M^{2+}]_C$, can be calculated from the ϕ_O determined from the ΔV_a. When comparing the magnitudes of currents measured in different solutions, assumption *a* requires that currents be compared at potentials V_M that are the same relative to V_a. In this way, the currents are being compared for a constant number of open channels and a constant V_C. For all the *I-V* curves measured, the maximum inward current occurred ~20 mV above V_a; therefore, we always used for comparison the current measured at $V_M = V_a + K$, where K is a constant for any one cell chosen such that $V_a + K$ is close to the potential at which the maximum current occurred in each solution. Values of K ranged from 17 to 24 mV. The current magnitudes at $V_a + K$, normalized by the current measured in the solution with 3 mM permeant ion, are plotted for Ca^{2+} in Fig. 2*C* and for Ba^{2+} in Fig. 3*C*. Note that while the Ca current only doubles in magnitude as the $[Ca^{2+}]_O$ increases from 1 to 30 mM, the Ba current increases by a factor of 4 for the same increase in $[Ba^{2+}]_O$.

To aid in the characterization of the dependence of Ca channel current on permeant ion species and concentration, we write the dependence of the Ca channel current, $I(M,C)$, on concentration as follows:

$$I(M,C) \propto A(M,C) * [M^{2+}]_C = A(M,C) * C * \exp[-2F\phi_O(M,C)/RT], \quad (4)$$

where $A(M,C)$ is a current-carrying-ability term dependent on both the species and concentration of the permeant ion, and C is $[M^{2+}]_O$. We introduce the cumbersome term "current-carrying ability" for $A(M,C)$ to distinguish this type of permeability from that defined by the reversal potential. Dividing Eq. 4 by the same expression for $C = 3$ mM gives:

$$I_n(M,C) \equiv \frac{I(M,C)}{I(M,3)} = \frac{A(M,C)}{A(M,3)} * \frac{C}{3} * \exp\{-2F[\phi_O(M,C) - \phi_O(M,3)]/RT\}. \quad (5)$$

$I_n(M,C)$ is the normalized current plotted in Figs. 2*C* and 3*C*, and $\phi_O(M,C) - \phi_O(M,3)$ is the ΔV_a plotted in Figs. 2*B* and 3*B*. Eq. 5 can be rewritten as:

$$\log[I_n(M,C)*3/C] = -0.87F*\Delta V_a(M,C)/RT - \log[A(M,3)/A(M,C)]. \quad (6)$$

If the current-carrying ability is independent of concentration, the second term on the right-hand side of Eq. 6 is zero; then $\log[I_n(M,C)*3/C]$ would be linearly related to $\Delta V_a(M,C)$ with a slope of $-1/29$ mV.

I_n*3/C is plotted against ΔV_a on semilog plots for Ca^{2+} (Fig. 4*A*) and Ba^{2+} (Fig. 4*B*). The straight line drawn in each plot has a slope of $-1/29$ mV. The Ba data

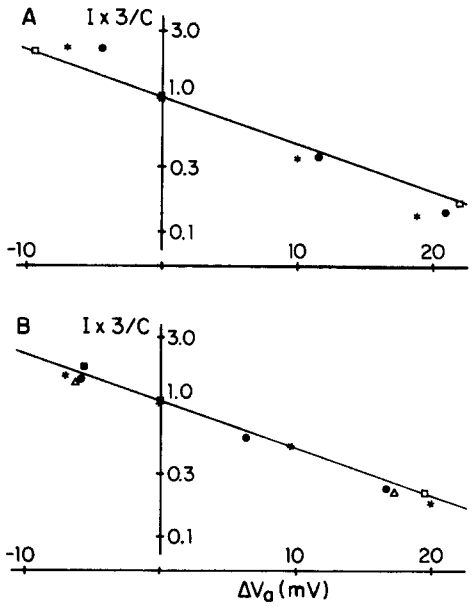

FIGURE 4. Dependence of Ca channel current on the concentration of permeant ion at the mouth of the channel, $[M^{2+}]_C$, assuming the pore sees the same surface potential. Data are from the experiments reported in Figs. 2 and 3. (*A*) Ratio of Ca current to $[Ca^{2+}]_O$ vs. surface potential shift. The ordinate is the normalized current at $V_a + K$ (Fig. 2*C*) divided by $[Ca^{2+}]_O/3$; ΔV_a (Fig. 2*B*) is the abscissa. The straight line has a slope of $-1/29$ mV and shows the relation expected if the current is proportional to the $[Ca^{2+}]_C$. (*B*) Ratio of Ba current to $[Ba^{2+}]_O$ vs. surface potential shift. The ordinate is the normalized current at $V_a + K$ (Fig. 3*C*) divided by $[Ba^{2+}]_O/3$; ΔV_a (Fig. 3*B*) is the abscissa. The straight line has a slope of $-1/29$ mV.

fit the straight line reasonably well, which implies that the ability of the Ca channel to carry Ba current is independent of concentration for this range of concentrations. However, the Ca data deviate from the straight line in a manner which implies that the current-carrying ability of Ca^{2+} tends to drop as concentration increases, i.e., there is a saturation of the Ca current.

Another way to demonstrate the dependence of the Ca channel current on concentration is to calculate $[M^{2+}]_C$ from $[M^{2+}]_O$ and ϕ_O. This approach is

dependent on the additional assumptions we made in order to calculate ϕ_O for Ba solutions using the Grahame equation (Eq. 3). The values for ϕ_O in Ca solutions are obtained from the ϕ_O values for Ba solution and the ΔV_a for changes between Ca and Ba solutions (see below). Fig. 5*A* shows the calculated relations between $[M^{2+}]_C$ and $[M^{2+}]_O$ for Ca^{2+} and Ba^{2+}. The normalized current is plotted against $[M^{2+}]_C$ for Ca^{2+} in Fig. 5*B* and for Ba^{2+} in Fig. 5*C*. The linear relation between Ba current and concentration and the presence of saturation for the Ca

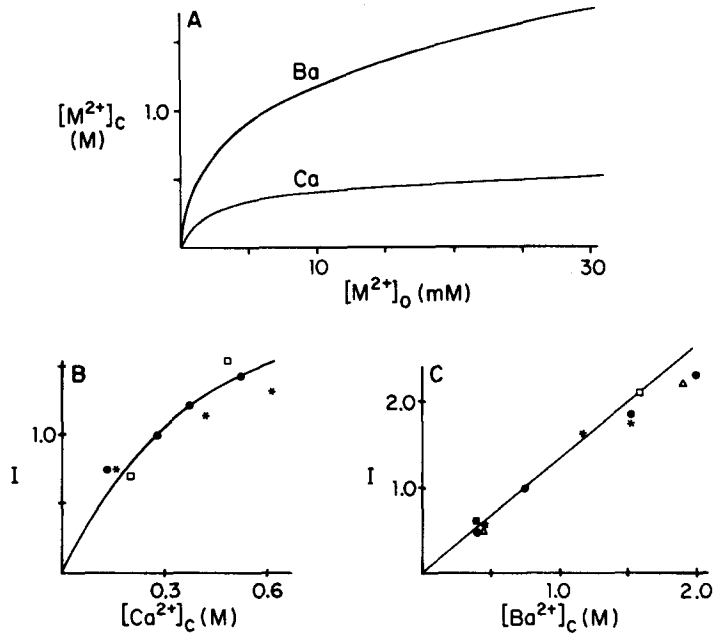

FIGURE 5. Dependence of Ca channel current on the concentration of permeant ion at the mouth of the channel, $[M^{2+}]_C$, assuming the pore sees the surface potential. Data are from the experiments reported in Figs. 2 and 3. (*A*) Calculated relation between the surface permeant ion concentration $[M^{2+}]_C$ and the bulk concentration $[M^{2+}]_O$. The surface concentrations are calculated using Eq. 1 and the absolute surface potentials fitted to the data in Fig. 3*B* (Grahame equation) and the ΔV_a values from Figs. 2*B* and 7*B*. (*B*) Dependence of Ca current on $[Ca^{2+}]_C$. The curve was drawn through the data by eye. (*C*) Dependence of Ba current on $[Ba^{2+}]_C$. The straight line is drawn from the origin to the point for $[Ba^{2+}]_O$ = 3 mM, which is the reference for the current normalization.

current is quite clear in these plots. The Ca current saturation has a dissociation constant K_D around $[Ca^{2+}]_C$ = 0.3 M, which corresponds to $[Ca^{2+}]_O$ = 3 mM. Actually, the data for higher Ba^{2+} concentrations (Fig. 5*C*) are suggestive of the beginning of saturation, but the K_D for Ba^{2+} is larger than that for Ca^{2+}.

Now we return to assumption *b*, that the mouth of the channel sees none of the surface potential. Since under this assumption the potential seen by the permeation mechanism is equal to the measured transmembrane potential, V_M

(except for a possible constant internal surface potential), currents flowing in different solutions are most easily compared by measuring currents for a constant V_M and then correcting for the different amounts of activation expected at that V_M in the different solutions. We calculate the activation corrections, using the activation curve for 30 mM Ca^{2+} shown in Fig. 1*A* and the changes in surface potential for the different solutions plotted in Figs. 2*B* and 3*B*. With assumption *b*, the concentration of permeant ion at the mouth of the channel is the same as the bulk concentration. Fig. 6 shows the current-concentration relations obtained from Ca and Ba currents in this manner. In Fig. 6*A*, the Ca currents measured

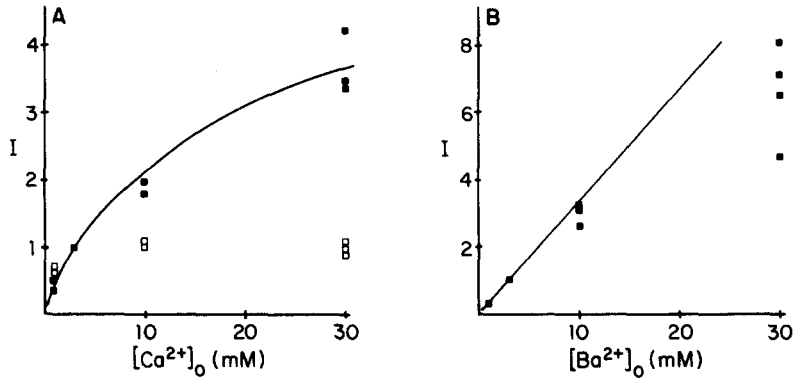

FIGURE 6. Dependence of Ca channel current on the concentration of permeant ions at the mouth of the channel, $[M^{2+}]_C = [M^{2+}]_O$, assuming the pore does not see the surface potential. Data are from the experiments reported in Figs. 2 and 3. All the data of Fig. 5 are included here, but there is a considerable overlap of points. (*A*) Dependence of Ca current on $[Ca^{2+}]_O$. Open symbols give the currents measured at +20 mV, without correction. Filled symbols give the currents measured at +20 mV, corrected for the reduced fraction of channels activated at +20 mV in higher Ca solutions caused by the surface potential shift. The curve is drawn through the corrected data by eye. (*B*) Dependence of Ba current on $[Ba^{2+}]_O$. All currents are measured at +10 mV and corrected for the variable fraction of channels activated at +10 mV caused by the surface potential shifts seen by the gating mechanism. The straight line is drawn from the origin to the point for $[Ba^{2+}]_O$ = 3 mM, which is the reference for the current normalization.

at +20 mV are plotted before (open squares) and after (closed squares) the correction for shifts of activation voltage dependence. It can be seen that the activation correction changes the current-concentration relation from one that would suggest total saturation to one that has a strong concentration dependence. The Ba current increases with concentration in a fashion which is considerably more linear than that for the Ca current. A comparison of Fig. 6, *A* and *B*, with Fig. 5, *B* and *C*, shows that the shapes of the current-concentration relations are roughly the same for either assumption (*a* or *b*). For this range of bulk solution concentrations, Ba currents are almost linearly related to concentration, while Ca currents show moderate saturation. Since activity coefficients would be expected to decrease with concentration for this range of bulk concentrations, plots of current vs. activity would show even less saturation.

Relative Permeability of Divalent Cations through Ca Channel

RELATIVE CURRENT-CARRYING ABILITY One way of characterizing the selectivity of the Ca channel permeation mechanism is to compare the size of the inward currents obtained when different species of divalent cations are used for the permeant ion (see Hagiwara and Byerly, 1981, for a review). The term $A(M,C)$ in Eq. 4 defines permeability in this sense. Fig. 7 *A* shows the *I-V* relations determined in one cell for Ca, Ba, and Sr currents, where in each case the

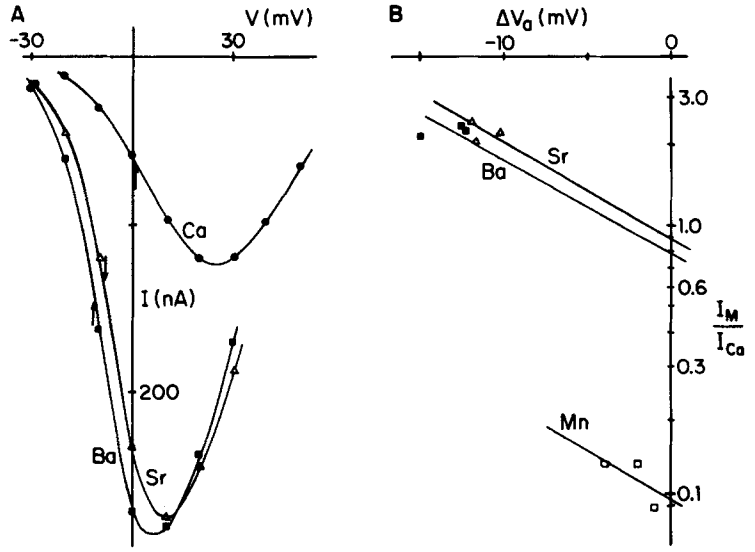

FIGURE 7. Selectivity of Ca channel for Ca^{2+}, Ba^{2+}, Sr^{2+}, and Mn^{2+}. Permeation experiment: small-opening suction electrode, intracellular microelectrode, room temperature. The pulse duration was 30 ms and the holding potential was −50 mV. The internal solution was Cs-aspartate; external solutions were 10 mM Ca (●), 10 mM Ba (■), 10 mM Sr (△), and 10 mM Mn (□) salines. (*A*) Peak Ca channel current plotted against pulse potential. Arrows indicate V_a values. Mn currents were not measured for this cell. (*B*) Plot of normalized current vs. change in surface potential. The ordinate is the Ca channel current at $V_a + K$; the abscissa is the shift of V_a relative to the V_a for 10 mM Ca saline. Data for each ion (Ba^{2+}, Sr^{2+}, and Mn^{2+}) have been obtained from three different cells. The straight lines of slope −1/29 mV have been drawn through the mean of the data for each ion. The intersections of these lines with the ordinate axis give the relative magnitudes of the currents that these ions would be expected to carry when their concentrations at the channel mouth are equal to that of Ca^{2+} in 10 mM Ca saline, assuming the pore sees the surface potential shift.

permeant ion concentration was 10 mM. It can be seen that the maximum inward current was about twice as large for Ba or Sr as it was for Ca. However, V_a was 10–15 mV more positive for Ca than for Ba or Sr; so relative current-carrying abilities cannot be determined until corrections are made for the shifts in surface potential. Assuming that the mouth of the channel sees the same surface potential shift (assumption *a*), currents were measured at V_a + K (approximately the

maximum currents) and the concentration of Ca^{2+} at the mouth of the channel was calculated to be considerably lower than that of Ba^{2+} or Sr^{2+}. If $A(M,C)$ is independent of C, Eq. 4 predicts that $I(M,C)$ will decrease by a factor of 10 for a 29-mV shift of V_a in the positive direction. In Fig. 7*B*, the currents carried by Ba^{2+}, Sr^{2+}, and Mn^{2+} are divided by the Ca current and plotted against the surface potential shift, ΔV_a, on a semilog plot; all currents are measured at $V_a + K$ with solutions containing 10 mM of the permeant ion. The intercept of a straight line drawn through the data with a slope of $-1/29$ mV with the current axis gives the size of the current that would be carried by that ion relative to that of the Ca current with equal concentration at the channel opening, assuming the current-carrying ability is independent of concentration. The ratio of currents obtained with equal surface concentrations is the relative current-carrying ability $A(M)/A(Ca)$. We have shown that $A(Ba)$ is nearly independent of concentration (Figs. 4*B* and 5*C*) and $A(Sr)$ is probably independent also, given the near equality of Ba and Sr currents in all cases studied. Therefore, the *y*-intercepts of the lines drawn through the Ba and Sr data in Fig. 7*B* indicate that the current-carrying abilities of the *Lymnaea* Ca channel for Ca^{2+}, Sr^{2+}, and Ba^{2+} are roughly equal, being 1.0, 0.9, and 0.8, respectively. Given the scatter in the data and the small sample, these differences in current-carrying ability are probably not significant.

When external Ca^{2+} is replaced by Mn^{2+}, small inward currents are recorded with almost the same voltage dependence as the Ca current. These data have also been included in Fig. 7*B*. Given the small values of ΔV_a involved, the projection to $\Delta V_a = 0$ is not important, and it is clear that the ability of the Ca channel to carry Mn current is only ~1/10 of that to carry Ca current.

If instead it is assumed that the mouth if the channel sees no surface potential (assumption *b*), the currents of Fig. 7*A* are measured at a fixed potential (+20 mV) and then corrected for the unequal activation caused by the surface potential shifts. In this way, we obtained $A(Ba)/A(Ca)$ equal to 0.9 ± 0.2 for four cells and $A(Sr)/A(Ca)$ equal to 1.2 ± 0.1 for three cells. So, with either assumption as to the amount of surface potential at the pore opening, the Ca channel is found to let Ca^{2+}, Sr^{2+}, and Ba^{2+} pass through almost equally well.

PERMEABILITY MEASURED FROM REVERSAL POTENTIAL When the current passing through the channel of interest can clearly be seen to reverse at a particular potential, permeability is usually defined by the expression derived in constant field theory that relates the reversal potential to the permeabilities and concentrations of permeant ions. This definition of permeability can give relative permeabilities for permeant ions that are very different from the relative current-carrying abilities (Hagiwara et al., 1971; Hille, 1975). Recently, reversal of the current passing through the Ca channel has been reported for heart cells (Lee and Tsien, 1982), chromaffin cells (Fenwick et al., 1982), and lymphocytes (Fukushima and Hagiwara, 1984). In snail neurons, the presence of several overlapping outward currents at large positive potentials has made any outward current that may pass through the Ca channel very difficult to identify. In an effort to measure reversal potentials for the Ca channel, we measured *I-V* relations before and after application of 0.1 mM Cd^{2+} or before and after Ca

current decay, while perfusing the cell with a highly buffered internal solution of pH 8.2. The high internal pH greatly suppresses the H^+ currents that are activated at positive potentials (Byerly et al., 1984*b*). We hoped to a see a reversal when we used only 1 mM Ba^{2+} for the external permeant ion, since Lee and Tsien (1982) found that the outward movement of Cs^+ through the Ca channel could be seen better when the external solution contained Ba^{2+} instead of Ca^{2+}. Hess and Tsien (1983) have reported that Na^+ moves out through the Ca channel better than Cs^+. Unfortunately, we found that our snail neurons deteriorated rapidly when they were internally perfused with pH 8.2 Na-aspartate, as judged by the continuously increasing inward holding current and decreasing membrane resistance. When internally perfused with pH 8.2 Cs-aspartate, the resting membrane resistance and holding current were stable throughout the experiments.

The currents recorded in these experiments did not show a clean reversal of current through the Ca channel. The shape of the currents did not reverse. As shown in Fig. 8*A*, at lower potentials (0–20 mV) the inward Ba current appeared to inactivate during the pulse, while at higher potentials (70–90 mV) an outward current slowly activated during the pulse. Currents were measured at 5 ms to minimize contamination by the slowly activating outward current, which is presumably unrelated to the Ca channel. The *I-V* curves measured after either Ca current decay or application of 0.1 mM Cd^{2+} were indistinguishable; no inward current was present and the outward current was suppressed. With 1 mM Ba saline, the before and after *I-V* curves always intersected near 50 mV (Fig. 8*C*); the intersection potential was 48.3 ± 1.3 mV (mean ± SD, $n = 4$). The outward current remaining at large positive potentials after Cd^{2+} application or Ca current decay had the same time course that was seen at those potentials before the Cd^{2+} application or decay. When the external solution contained 1 mM Ca^{2+} instead of Ba^{2+}, the results were very similar, except that the intersection potential was 60.4 ± 2.9 mV ($n = 4$). When the external Ba^{2+} concentration was increased to 10 mM (Fig. 8*B*), the before and after *I-V* curves nearly superimposed between 80 and 100 mV, so that an intersection was poorly defined (Fig. 8*D*). The intersection potential determined from three cells was 90 ± 10 mV.

Although these intersection potentials could be interpreted as reversal potentials for the Ca channel current (which implies that Ca^{2+} is more permeant than Ba^{2+}), they might be determined by the summing of two independent nonreversing currents—an inward divalent current that decreases with potential and an outward current that increases with potential and is also sensitive to Cd^{2+} and washout. In this latter interpretation, the 12-mV shift of the intersection potential caused by replacing Ba^{2+} with Ca^{2+} is expected from the change in surface potential discussed above (Fig. 7). It is interesting that increasing the Ba^{2+} concentration by a factor of 10 shifts the intersection potential 40 mV in the positive direction and practically eliminates the intersection.

Since it is not clear if a reversal potential for the Ca channel current can be measured in *Lymnaea* neurons, we only have confidence in the permeabilities determined from current magnitude (current-carrying abilities). This will probably be the case for the Ca channel current in a number of different tissues.

Interactions Between Species of Divalent Cations

RELATIVE EFFICACY OF CALCIUM CHANNEL BLOCKERS Ca channels can also be characterized by their sensitivity to different blocking agents. We studied the blocking effect of three divalent cations, Cd^{2+}, Co^{2+}, and Ni^{2+}, on the Ca current of *Lymnaea* neurons. Cd^{2+} blocks the Ca current at concentrations two orders of

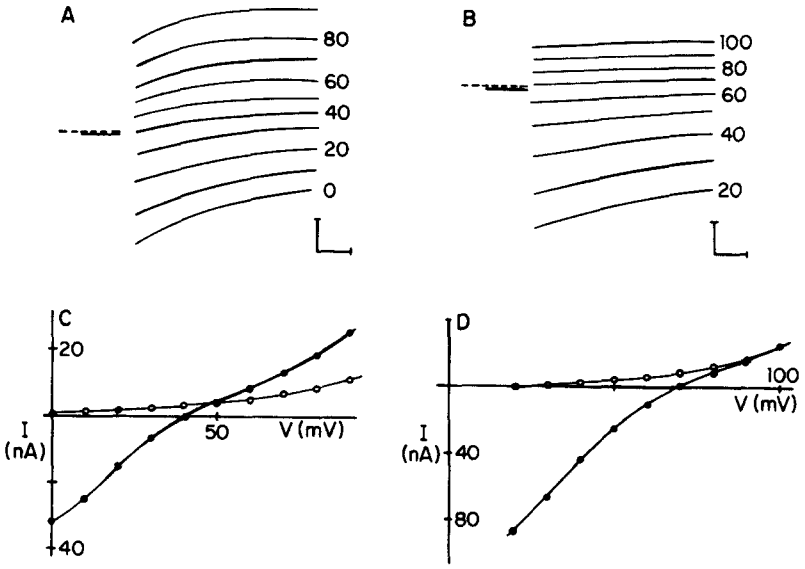

FIGURE 8. Reversal of current. Reversal experiment: large-opening suction electrode, no intracellular electrode, room temperature. The pulse duration was 60 ms and the holding potential was −60 mV. Linear leakage and capacitive currents have not been subtracted. The internal solution is pH 8.2 Cs-aspartate. (*A* and *B*) Tracings of current records obtained with 1 mM Ba (*A*) and 10 mM Ba (*B*) salines. The current records are contaminated with capacitive currents during the first few milliseconds (Byerly and Hagiwara, 1982) and have not been copied for the first 5 ms following the beginning of the pulse. The amplitude of the pulse was increased by steps of 10 mV; numbers to the right of current records give the potentials (millivolts) reached by the pulses. Dashed lines indicate the zero current level. Holding currents are −0.6 (*A*) and −1.0 nA (*B*). Calibration bars are 10 nA × 10 ms (*A*) and 20 nA × 10 ms (*B*). (*C* and *D*) *I-V* curves for currents before (●) and after (○) adding 0.1 mM Cd^{2+} to the external solution. Current was measured at 5 ms or earlier if a more negative current was recorded before 5 ms. In *C*, the external solution was 1 mM Ba saline and the before data (●) come from the records shown in *A*. In *D*, the external solution was 10 mM Ba saline and the before data come from the records shown in *B*.

magnitude lower than those required for Co^{2+} or Ni^{2+} to block the current (Fig. 9). The data plotted in Fig. 9 show the magnitude of the peak Ca current in the presence of the indicated concentration of blocker divided by the Ca current magnitude in the absence of blocker. These measurements for *Lymnaea* were made in solutions containing 4 mM Ca^{2+} and 4 mM Mg^{2+}. Since there was no

significant shift of the Ca current *I-V* curve until the blocker concentration exceeded 1 mM, the reduction in Ca current is due to a blocking effect, not to a reduction of $[Ca^{2+}]_C$ resulting from a change in surface potential. The data are fitted reasonably well by the curves drawn according to one-to-one binding. The apparent dissociation constants, K_D, determined for Cd^{2+}, Ni^{2+}, and Co^{2+} are 3×10^{-6}, 6×10^{-4}, and 9×10^{-4} M, respectively. These data and those from blocker studies done on many other neurons all agree with the same pattern of sensitivity to these blockers. It seems reasonable to conclude that all *Lymnaea* neurons have the same type of Ca channel with respect to blocker sensitivity.

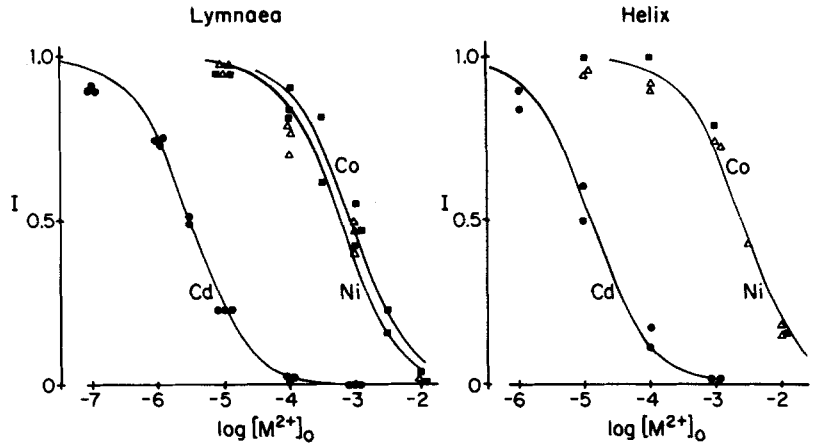

FIGURE 9. Dose-response curves for block of Ca current by Cd^{2+} (●), Ni^{2+} (△), and Co^{2+} (■). Blocker experiments: small-opening suction electrode, no intracellular microelectrode, and room temperature. Currents were measured at the potential that gave the largest inward current and the linear leakage current was subtracted. All currents are expressed as the fraction of the maximum current recorded before the addition of blocker. Curves show the relation expected for one-to-one binding; apparent K_D values are given in the text. *Lymnaea:* the external solution was Tris saline (4 mM Ca^{2+}) and the internal solution was Cs-aspartate. Data were taken from three cells for each of the blocking ions. *Helix:* the external solution was *Helix* Tris saline (10 mM Ca^{2+}) and the internal solution was *Helix* Cs-aspartate. Data were taken from two cells for Cd^{2+}, two for Ni^{2+}, and one for Co^{2+}.

Since very different sensitivities to these blocking ions have been reported for neurons of other species of snail, we repeated the study of the blocking action of Cd^{2+}, Co^{2+}, and Ni^{2+} on neurons from *Helix aspersa*. The results of this study are also given in Fig. 9 and show the same relative sensitivities that were found for *Lymnaea*; Co^{2+} and Ni^{2+} are equally effective and Cd^{2+} blocks at concentrations two orders of magnitude smaller. The K_D for Cd^{2+} is 1.3×10^{-5} M and that for Ni^{2+} and Co^{2+} is 2.5×10^{-3} M. The increase by a factor of 4 in the dissociation constants between species is not surprising, since *Helix* saline contains a higher concentration of Ca^{2+} (10 mM) and Ca^{2+} competes with the blocking ion, as shown below. Thus, the Ca channels of *Helix* neurons and *Lymnaea* neurons appear to have the same sensitivities to blocking ions.

The organic Ca channel blockers verapamil and nifedipine are potent blockers of Ca current in heart and smooth muscle (Fleckenstein, 1977; Rosenberger and Triggle, 1978). In earlier experiments, we had found that concentrations of verapamil as high as 1 mM had only weak, if any, blocking action on the *Lymnaea* Ca current. Those experiments were done on well-perfused neurons; in the presence of Ca current washout, it was impossible to quantify the effect of verapamil. In this study, we tested the action of nifedipine on poorly perfused *Lymnaea* neurons, as was done in the above studies with Cd^{2+}, Co^{2+}, and Ni^{2+}. The action of nifedipine was weak, slow, and largely irreversible. When 10^{-4} M nifedipine was added to the bath solution, the Ca current began to decline slowly,

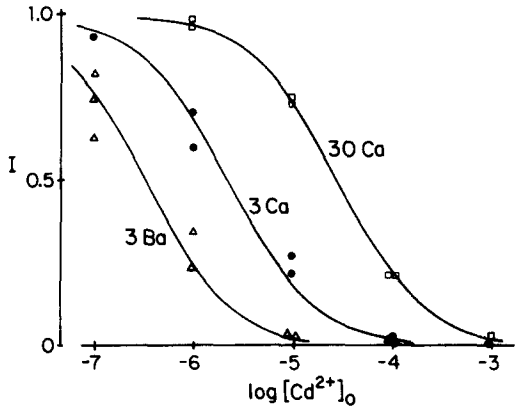

FIGURE 10. Cd dose-response curves for different species and concentrations of permeant ions. Permeation experiments: small-opening suction electrode, intracellular microelectrode, and room temperature. External solution was 3 mM Ca saline (●), 30 mM Ca saline (□), or 3 mM Ba saline (△). The internal solution was Cs-aspartate. Currents were measured at the potential that gave the largest inward current; the linear leakage current was eliminated by the addition of currents from equal and opposite voltage pulses. All currents are expressed as the fraction of the maximum current recorded before the addition of Cd^{2+}. Curves show relations expected for one-to-one binding; apparent K_D values are given in the text.

as determined by test pulses to +20 mV applied once per minute. Even after a 15-min exposure to nifedipine, a steady state had not been reached and only 30–40% of the Ca current was blocked. This slow effect is in sharp contrast to the blocking action of the divalent cations, which reaches a steady state within a few seconds of the time of addition of the blocker to the bath. The blocking action of nifedipine was not increased by more frequent stimulation.

DEPENDENCE OF BLOCKING ON PERMEANT ION The concentration of a blocker required to block the Ca channel current depends on the species and concentration of the permeant ion. This is demonstrated for the blocking action of Cd^{2+} in Fig. 10. Cd^{2+} is more effective in blocking Ba current than Ca current with equal permeant ion concentrations, and Cd^{2+} is less effective in blocking the Ca current when $[Ca^{2+}]_o$ is increased. The apparent dissociation constants

determined for Cd^{2+} block are 3.3×10^{-7}, 2.2×10^{-6}, and 2.8×10^{-5} M for 3 mM Ba^{2+}, 3 mM Ca^{2+}, and 30 mM Ca^{2+}, respectively. These changes in the efficacy of Cd^{2+} blocking can be explained partially by the changes in surface potential that accompany the changes in $[M^{2+}]_o$, assuming the mouth of the channel sees the same surface potential that is seen by the gating mechanism. Since V_a shifts 20 mV in the positive direction when $[Ca^{2+}]_o$ is changed from 3 to 30 mM (Fig. 2), the concentration of Cd^{2+} at the channel would be reduced

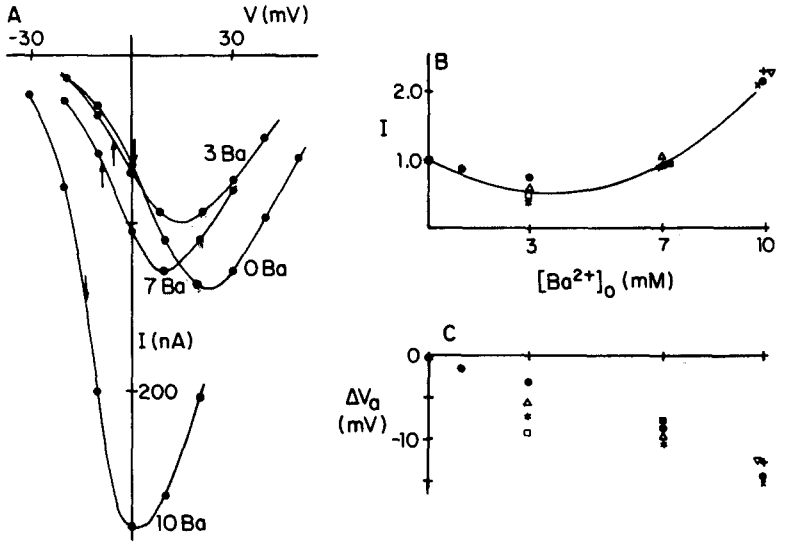

FIGURE 11. Anomalous mole fraction effect for mixtures of Ba^{2+} and Ca^{2+}. Permeation experiments: small-opening suction electrode, intracellular microelectrode, and room temperature. Each external solution contained a 10-mM concentration of Ba^{2+} and Ca^{2+}; the solutions are identified by their concentration of Ba^{2+}. (*A*) *I-V* curves measured in one cell for four different external solutions. External solutions were 10 mM Ba, 7 mM Ba/3 mM Ca, 3 mM Ba/7 mM Ca, and 10 mM Ca salines. Arrows indicate V_a values. (*B*) Relative current magnitude vs. Ba/Ca composition of solutions. Currents are measured at $V_a + K$ (K is ~20 mV) and expressed as a ratio to the current measured for that cell with 10 mM Ca saline. Different symbols are used to plot data from different cells; a total of eight cells were studied. The curve is drawn through the data by eye. (*C*) Shifts of V_a vs. Ba/Ca composition of solutions. Shifts are measured relative to the V_a determined for that cell in 10 mM Ca saline.

by a factor of 5 in the 30 mM Ca solution. Similarly, the 12-mV shift of V_a in the negative direction for changing from 3 mM Ca saline to 3 mM Ba saline would predict a 2.5-times increase in the concentration of Cd^{2+} at the channel. However, the K_D for 30 mM Ca saline is actually 13 times that for 3 mM Ca saline and the K_D for 3 mM Ba saline is reduced by a factor of 7. Therefore, it appears that the permeant ion competes with Cd^{2+} at the blocking site, and that Ca^{2+} competes more strongly than does Ba^{2+}.

ANOMALOUS MOLE FRACTION EFFECT It is well known that some divalent ions which block Ca current can themselves carry current through the Ca channel, e.g., Mn^{2+} and Cd^{2+} (see Hagiwara and Byerly, 1981). Recently, it has been shown that Ca^{2+} itself can exert a blocking effect on Ca channel current. Hess and collaborators (1983) reported that Ca^{2+} exerted a blocking effect on the Ba^{2+} current in heart cells, either when the concentration of Ba^{2+} was held constant or when the sum of the concentrations of Ba^{2+} and Ca^{2+} was held constant. In the latter type of experiment, the reduction in Ca channel current for mixtures of Ba^{2+} and Ca^{2+} relative to that obtained with either ion alone is called an "anomalous mole fraction effect," a term used to describe a similiar

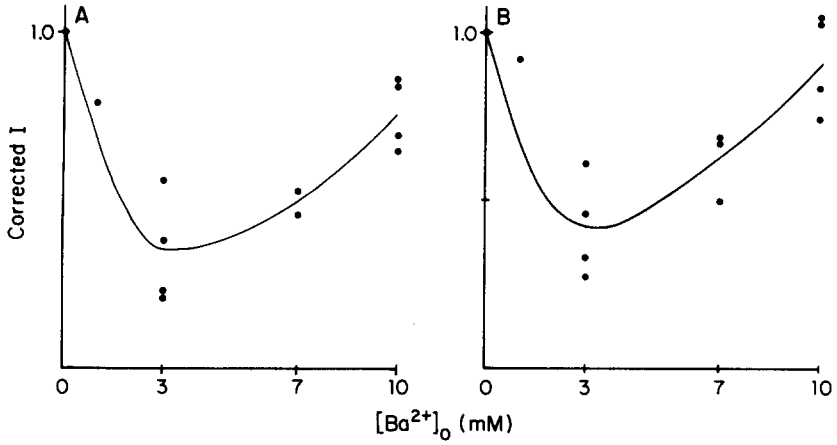

FIGURE 12. Anomalous mole fraction data corrected for changing surface potential effects. All external solutions contain a 10-mM concentration of Ca^{2+} and Ba^{2+} and are identified by their concentrations of Ba^{2+}. The corrected currents are normalized to the current obtained in 10 mM Ca saline. The curves are drawn through the data by eye. (*A*) Dependence of current on mole fraction, assuming the pore sees the surface potential. Corrected currents are obtained by dividing the currents of Fig. 11*B* by the total concentration of Ba^{2+} and Ca^{2+} at the channel opening. (*B*) Dependence of current on mole fraction, assuming the pore sees no surface potential. Currents measured at +20 mV are corrected for the variable activation caused by the measured surface potential shifts (Fig. 11*C*).

phenomenon with the inward rectifying K channel (Hagiwara and Takahashi, 1974). We also saw an anomalous mole fraction effect with the *Lymnaea* Ca channel, although its presence was somewhat obscured by the changing surface potential. Fig. 11*A* shows the *I-V* curves obtained for two mixtures of Ca^{2+} and Ba^{2+}, as well as those for only Ca^{2+} and for only Ba^{2+}; the total concentration of Ca^{2+} and Ba^{2+} was 10 mM in all solutions. While the surface potential changes monotonically as Ba^{2+} is substituted for Ca^{2+} (Fig. 11*C*), the peak current goes through a minimum when there is 3 mM Ba^{2+} outside the cell (Fig. 11*B*). In order to determine how the Ca channel current depends on the mole fraction for a constant transmembrane potential and constant concentration of permeant

ions at the pore opening, we have corrected the data, using either assumption *a* or *b*. Following assumption *a*, increases in $[Ba^{2+}]_o$ are accompanied by increases in the total concentration of Ba^{2+} and Ca^{2+} at the mouth of the channel caused by the changing surface potential. The currents of Fig. 11*B*, which are measured at fixed potentials relative to V_a, have been divided by the calculated total surface concentration of Ca^{2+} and Ba^{2+} to give corrected currents, which are plotted in Fig. 12*A*. Fig. 12*B* shows the dependence of Ca channel current on the mole fraction that is obtained if assumption *b* is made. Currents measured at +20 mV are corrected for the different amounts of activation in the different solutions expected from the measured shifts in surface potential. As can be seen, both assumptions give similar results. The anomalous mole fraction effect is even more prominent in the corrected data; the current for the solution containing 7 mM Ca^{2+} and 3 mM Ba^{2+} is <50% of the currents obtained with all Ca^{2+} or all Ba^{2+}. External Ba^{2+} appears to block the Ca current and external Ca^{2+} appears to block Ba current, the former effect being somewhat stronger than the latter. An anomalous mole fraction effect was not found for mixtures of Ba^{2+} and Sr^{2+}. The corrected Ca channel current measured with external solutions containing 5 mM Ba^{2+} and 5 mM Sr^{2+} was the same size as that measured with 10 mM Ba^{2+} in the external solution.

DISCUSSION

Surface Potential

The data presented in this and previous papers (Byerly and Hagiwara, 1982; Byerly et al., 1984*a*) are consistent with the interpretation that the gating mechanism of the Ca channel sees a change in the external surface potential when the concentration or species of the divalent cation is changed. However, it is not known if the pore of the channel also sees this surface potential. We have found that after correction for surface potential effects, the current-concentration relations (Figs. 5 and 6), relative current-carrying abilities (Fig. 7), and mole fraction relations (Fig. 12) are qualitatively the same for either of two assumptions: (*a*) the pore sees the same surface potential that the gating mechanism sees, or (*b*) the pore sees none of the surface potential. The insensitivity of our conclusions to the particular assumption used is at first surprising, but is explained simply. If a change of the external solution makes the external surface potential (seen by the gating mechanism) more negative, then both assumptions predict an increase (of about the same size) in the single channel current. Consider the single channel current measured at a fixed potential as seen by the gating mechanism, i.e., at $V_a + K$. According to assumption *a*, the potential across the pore is unchanged at $V_a + K$, but the concentration of permeant ions at the mouth of the pore is increased by the Boltzmann factor. According to assumption *b*, the potential across the pore becomes more negative, but the concentration of permeant ions at the mouth of the pore is unchanged. If the change in surface potential is −15 mV, the Boltzmann factor is ~3. The voltage dependence of the single channel current has only been measured for 4 mM Ca^{2+} or Ba^{2+} in the external solution (Byerly et al., 1984*a*); these data give a twofold increase for a

15-mV negative shift in the range of voltages where our measurements are made. Therefore, the change in current magnitude caused by the change in surface potential will be similar whether the mouth of the pore sees the surface potential or not. Given the present uncertainty about the single channel current-voltage relation for the Ca channel, it seems very difficult to determine experimentally if the mouth of the channel sees the surface potential.

Relative Permeabilities

We found that Ca^{2+}, Sr^{2+}, and Ba^{2+} carried current through the Ca channel about equally well. This agrees with the conclusion of Wilson et al. (1983) that the permeabilities (current-carrying abilities) of the *Helix* Ca channel for Ca^{2+}, Sr^{2+}, and Ba^{2+} are equal. The equal permeabilities that are observed in snail neurons are in contrast to the considerably reduced relative permeabilities found for Ba^{2+} and Sr^{2+} in tunicate oocyte membrane; the Ca:Sr:Ba permeabilities were 1.0:0.56:0.21 (Ohmori and Yoshii, 1977) or 1.0:0.66:0.26 (Okamoto et al., 1977). Okamoto and co-workers (1977) also studied the relative permeabilities of Ca^{2+}, Sr^{2+}, and Ba^{2+} in sea urchin and mouse eggs and concluded that they were essentially the same as those for tunicate egg. Hagiwara and Ohmori (1982) found that rat clonal pituitary cells (GH_3) had Ca channels with higher permeabilities for Ba^{2+} and Sr^{2+} than for Ca^{2+}; the Ca:Sr:Ba sequence was 1.0:1.6:2.7. In this case, all three divalent ions seem to exert only screening effects on the surface charge (no binding), so relative permeabilities are obtained directly from current magnitudes. Thus, the relative permeabilities suggest that these Ca channels fall into three classes: egg Ca channels in which Ba^{2+} carried less than half the current carried by Ca^{2+}, snail neuron Ca channels in which Ba^{2+} carries about the same current as does Ca^{2+}, and rat pituitary Ca channels in which Ba^{2+} carries more than twice the current carried by Ca^{2+}. In all cases, the Sr permeability is intermediate to the Ca and Ba permeabilities.

Blocker Action

Our studies of the blocking efficacy of Cd^{2+}, Ni^{2+}, and Co^{2+} suggest that all Ca channels in neurons of the snails *Lymnaea* and *Helix* have the same sensitivities to these blocking cations, although the K_D values for *Helix* are about four times larger, presumably because of the higher $[Ca^{2+}]_O$. For both species, Cd^{2+} is effective at concentrations 200 times smaller than those required for Ni^{2+} or Co^{2+}. Our results are not in agreement with those reported by Akaike et al. (1978) for *Helix aspersa*. They found Cd^{2+} and Co^{2+} to be about equally effective but 100 times less effective than Ni^{2+}. Kostyuk et al. (1977) reported a K_D for the blocking action of Cd^{2+} in *Helix pomatia* of 7.2×10^{-5} M, which is a factor of 5 larger than we found for *Helix aspersa* and a factor of 50 smaller than that found by Akaike et al. (1978). We know of no studies that determine the relative efficacy of all three of these blocking cations for other Ca channels. In barnacle muscle, the K_D for Co^{2+} blocking was a factor of ~4 smaller than that for Ni^{2+} (Hagiwara and Takahashi, 1967). The relative blocking efficacy of various divalents may prove to be a useful way of classifying Ca channels, but at present too few data are available. The one clear distinction between classes of Ca

channels that is based on blockers is the sensitivity to organic blockers. The results of the study of the action of nifedipine reported here demonstrate that organic Ca current blockers are relatively ineffective in blocking the Ca currents of certain membranes (Hagiwara and Byerly, 1981); there is a recent report that the Ca current of *Helix* neuron is half blocked by 3 μM nifedipine (Nishi et al., 1983).

The blocking efficacy of Cd^{2+} is dependent on the concentration and species of the permeant ion. Cd^{2+} is more effective in blocking Ba current than Ca current and is more effective against Ca current when $[Ca^{2+}]_o$ is low than when it is high (Fig. 10). The change in surface potential associated with changing the concentration or species of the permeant ion might change the concentrations of Cd^{2+} at the channel in the right direction to explain the changes in blocking efficacy. However, the measured surface potentials shifts are only about half as large as would be necessary to account for the observed changes in Cd^{2+} blocking, even assuming the mouth of the channel sees the entire shift. Hagiwara and Takahashi (1967) first noted this competition between the blocking and permeant ion and accounted for it by assuming that both bind to the same site and that the affinity of Ba^{2+} for this site is lower than that of Ca^{2+}.

Anomalous Mole Fraction Effect

Anomalous mole fraction effects for mixtures of Ba^{2+} and Ca^{2+} have been found for the Ca channels of guinea pig ventricular cells (Hess et al., 1983) and of frog muscle (Almers and McCleskey, 1984). In both studies, the Ca channel current was measured at a fixed potential for all solutions, with a total concentration of Ca^{2+} and Ba^{2+} of 10 mM for each solution. The Ba current (recorded with 10 mM Ba^{2+}) was larger than the Ca current (recorded in 10 mM Ca^{2+}), but the current recorded with certain mixtures of Ba^{2+} and Ca^{2+} was only 60–70% of the Ca current. Hess and Tsien (1984) obtained the minimum current in solutions containing 1–3 mM Ca^{2+}. The data of Almers and McCleskey (1984) are consistent with a minimum in the same mole fraction range. However, since no measurements of shifts in surface potential were made in these studies, it is not clear to what extent the changes in current magnitudes are due to the changes in surface potential when Ba^{2+} is substituted for Ca^{2+}. Hess and Tsien also demonstrated the anomalous mole fraction effect in the single channel currents determined from ensemble fluctuation analysis of whole-cell recordings, and concluded that it does not result from changes in the probability of channels being open. Since they only reported single channel data for one mixture of Ba^{2+} and Ca^{2+}, these data do not determine the mole fraction at which the minimum occurs. The anomalous mole fraction effect we measured for *Lymnaea* (Fig. 11*A*) seems to differ from that found in guinea pig and frog in that the minimum current is observed in solutions with more Ca^{2+} than Ba^{2+} (7 mM Ca^{2+}/3 mM Ba^{2+}). When the currents are corrected for the changes in surface potential using either assumption as to the surface potential at the channel mouth (Fig. 12), it is clear that the change from 10 mM Ca^{2+} to 7 mM Ca^{2+}/3 mM Ba^{2+} reduces the Ca channel current more than the change from 10 mM Ba^{2+} to 3 mM Ca^{2+}/7 mM Ba^{2+} does, which suggests that Ba^{2+} has more of a blocking effect on the Ca current than Ca^{2+} does on the Ba current.

Permeation Models

Hille and Schwarz (1978) pointed out that multi-ion single-file pores could account for anomalous mole fraction effects. Using models of this type, Hess and Tsien (1983, 1984) described the Ca channel of heart muscle and Almers and McClesky (1984) described that of skeletal muscle. A symmetrical two-site model with repulsion between ions in doubly occupied channels could account for their observed anomalous mole fraction effects. In these models, the selectivity of the channel for divalents results from the strong binding (deep wells in the energy profile) for Ca^{2+} ($-15RT$) and Ba^{2+} ($-10RT$); monovalent cations bind much more weakly to the sites. The repulsion between ions in the channel allows large divalent currents that increase with concentration into the millimolar range, in spite of the strong binding. We have tried to describe our results by a single-file, two-site model similar to that of Hess and Tsien (1984) and Almers and McCleskey (1984); we ignored monovalents, since we have no data on monovalent currents. The model parameters (well depths, barrier heights, and repulsion term) are constrained to values that are consistent with the concentration dependences shown in Fig. 5. We can find parameters that give ~30% reduction of current for mixtures of Ba^{2+} and Ca^{2+} compared with the pure Ca current. However, the predicted minimum current always occurs for small amounts of Ca^{2+} in the mixture, as though Ca^{2+} blocked Ba current more than Ba^{2+} blocked Ca current, and does not agree with our data (Fig. 12). A more complicated multi-ion single-file pore will probably be able to account for our data, but we have not attempted such modeling because of our lack of data for monovalent currents through the Ca channel. Not only have we been unable to identify outward monovalent Ca channel currents at large positive potentials in the presence of Ca^{2+}, but we have also been unable to study monovalent Ca channel currents in the absence of Ca^{2+}, as has been done by others (Kostyuk and Krishtal, 1977; Almers et al., 1982, 1984; Kostyuk et al., 1983; Hess and Tsien, 1984; Fukushima and Hagiwara, 1984). We found that replacing all the extracellular Ca^{2+} with Mg^{2+} causes *Lymnaea* cell bodies to deteriorate too rapidly to allow any credible current measurements.

The disagreement between the details of the anomalous mole fraction effect found in *Lymnaea* neurons and those reported for heart and skeletal muscle should not obscure the basic agreement between our results and a model for the Ca channel of the multi-ion, single-file type. Even after corrections for the surface potential shifts, there is a clear anomalous mole fraction effect, and the current magnitude increases nearly linearly with concentration for very high concentrations of Ba^{2+} and Ca^{2+}. The multi-ion, single-file model is very attractive for its ability to produce anomalous mole fraction effects and to reconcile these current-concentration relations with the very high affinity of Ca^{2+} and Ba^{2+} for Ca channel sites (demonstrated by their blocking of monovalent currents).

We gratefully acknowledge the assistance of Susumu Hagiwara and George Augustine during the preparation of this manuscript.

This work was supported by U. S. Public Health Service grant NS15341 to L.B. and by

fellowships from the American Heart Association and the National Institutes of Health to J.R.S.

Original version received 26 June 1984 and accepted version received 10 December 1984.

REFERENCES

Akaike, N., K. S. Lee, and A. M. Brown. 1978. The calcium current of *Helix* neuron. *J. Gen. Physiol.* 71:509–531.

Almers, W., and E. W. McCleskey. 1984. Nonselective conductance in calcium channels of frog muscle: calcium-selectivity in a single-file pore. *J. Physiol. (Lond.).* 353:585–608.

Almers, W., E. W. McCleskey, and P. T. Palade. 1982. Frog muscle membrane: a cation-permeable channel blocked by micromolar external [Ca^{2+}]. *J. Physiol. (Lond.).* 332:52P–53P.

Almers, W., E. W. McCleskey, and P. T. Palade. 1984. A nonselective cation conductance in frog muscle membrane blocked by micromolar external calcium ions. *J. Physiol. (Lond.).* 353:565–583.

Begenisich, T. 1975. Magnitude and location of surface charges on *Myxicola* giant axons. *J. Gen. Physiol.* 66:47–65.

Brehm, P., and R. Eckert. 1978. Calcium entry leads to inactivation of calcium channel in *Paramecium*. *Science (Wash. DC).* 202:1203–1206.

Byerly, L., P. B. Chase, and J. R. Stimers. 1984*a*. Calcium current activation kinetics in neurones of the snail *Lymnaea stagnalis*. *J. Physiol. (Lond.).* 348:187–207.

Byerly, L., R. Meech, and W. J. Moody. 1984*b*. Rapidly activating hydrogen ion currents in perfused neurones of the snail, *Lymnaea stagnalis*. *J. Physiol. (Lond.).* 351:199–216.

Byerly, L., and S. Hagiwara. 1982. Calcium currents in internally perfused nerve cell bodies of *Limnea stagnalis*. *J. Physiol. (Lond.).* 322:503–528.

Byerly, L., and W. J. Moody. 1982. Intracellular pH changes in perfused snail neurons. *Biophys. J.* 37:181*a*. (Abstr.)

Byerly, L., and W. J. Moody. 1984. Intracellular calcium ions and calcium currents in perfused neurones of the snail *Lymnaea stagnalis*. *J. Physiol. (Lond.).* 352:637–652.

Cota, G., and E. Stefani. 1984. Saturation of calcium channels and surface charge effects in skeletal muscle fibres of the frog. *J. Physiol. (Lond.).* 351:135–154.

Fenwick, E. M., A. Marty, and E. Neher. 1982. Sodium and calcium channels in bovine chromaffin cells. *J. Physiol. (Lond.).* 331:599–635.

Fleckenstein, A. 1977. Specific pharmacology of calcium in myocardium, cardiac pacemakers, and vascular smooth muscle. *Annu. Rev. Pharmacol. Toxicol.* 17:149–166.

Fukushima, Y., and S. Hagiwara. 1984. Currents carried by monovalent cations through calcium channels in mouse neoplastic B lymphocytes. *J. Physiol. (Lond.).* 358:255–284.

Hagiwara, S., and L. Byerly. 1981. Calcium channel. *Annu. Rev. Neurosci.* 4:69–125.

Hagiwara, S., and H. Ohmori. 1982. Studies of calcium channels in rat clonal pituitary cells with patch electrode voltage clamp. *J. Physiol. (Lond.).* 331:231–252.

Hagiwara, S., and K. Takahashi. 1967. Surface density of calcium ions and calcium spikes in the barnacle muscle fibre membrane. *J. Physiol. (Lond.).* 50:583–601.

Hagiwara, S., and K. Takahashi. 1974. The anomalous rectification and cation selectivity of the membrane of a starfish egg cell. *J. Membr. Biol.* 18:61–80.

Hagiwara, S., K. Toyama, and H. Hayashi. 1971. Mechanisms of anion and cation permeation in the resting membrane of a barnacle muscle fiber. *J. Gen. Physiol.* 57:408–434.

Hess, P., K. S. Lee, and R. W. Tsien. 1983. Ion-ion interactions in the Ca channel of single heart cells. *Biophys. J.* 41:293*a*. (Abstr.)

Hess, P., and R. W. Tsien. 1983. Calcium channel permeability to divalent and monovalent cations. A model with two ion binding sites and ion-ion interaction. *Soc. Neurosci. Abstr.* 9:509.

Hess, P., and R. W. Tsien. 1984. Mechanism of ion permeation through calcium channels. *Nature (Lond.)*. 309:453–456.

Hille, B. 1975. Ionic selectivity of Na and K channels of nerve membranes. *In* Membranes: A Series of Advances. G. Eisenman, editor. Marcel Dekker, New York. 3:255–323.

Hille, B., and W. Schwarz. 1978. Potassium channels as multi-ion single-file pores. *J. Gen. Physiol.* 72:409–442.

Kostyuk, P. G., and O. A. Krishtal. 1977. Effects of calcium and calcium-chelating agents on the inward and outward current in the membrane of mollusc neurones. *J. Physiol. (Lond.)*. 270:569–580.

Kostyuk, P. G., O. A. Krishtal, and Y. A. Shakhovalov. 1977. Separation of sodium and calcium currents in the somatic membrane of mollusc neurones. *J. Physiol. (Lond.)*. 270:545–568.

Kostyuk, P. G., S. L. Mironov, P. A. Doroshenko, and V. N. Ponomarev. 1982. Surface charges on the outer side of mollusc neuron membrane. *J. Membr. Biol.* 70:171–179.

Kostyuk, P. G., S. L. Mironov, and Y. M. Shuba. 1983. Two ion-selecting filters in the calcium channel of the somatic membrane of mollusc neurons. *J. Membr. Biol.* 76:83–93.

Lee, K. S., and R. W. Tsien. 1982. Reversal of current through calcium channels in dialysed single heart cells. *Nature (Lond.)*. 297:498–501.

McLaughlin, S. G. A., G. Szabo, and G. Eisenman. 1971. Divalent ions and the surface potential of charged phospholipid membranes. *J. Physiol. (Lond.)*. 58:667–687.

Nishi, K., N. Akaike, Y. Oyama, and H. Ito. 1983. Actions of calcium antagonists on calcium currents in *Helix* neurons. *Circ. Res.* 52:53–59.

Ohmori, H., and M. Yoshii. 1977. Surface potential reflected in both gating and permeation mechanisms of sodium and calcium channels of the tunicate egg cell membrane. *J. Physiol. (Lond.)*. 267:429–463.

Okamoto, H., K. Takahashi, and N. Yamashita. 1977. Ionic currents through the membrane of the mammalian oocyte and their comparison with those in the tunicate and sea urchin. *J. Physiol. (Lond.)*. 267:465–469.

Rosenberger, L., and D. J. Triggle. 1978. Calcium, calcium translocation and specific calcium antagonists. *In* Calcium in Drug Action. G. B. Weiss, editor. Publishing Corp., New York. 3–31.

Tillotson, D. 1979. Inactivation of Ca conductance dependent on entry of Ca ions in molluscan neurons. *Proc. Natl. Acad. Sci. USA*. 76:1497–1500.

Wilson, D. L., K. Morimoto, Y. Tsuda, and A. M. Brown. 1983. Interaction between calcium ions and surface charge as it relates to calcium currents. *J. Membr. Biol.* 72:117–130.